



Lab on a Chip

Rapid and Inexpensive Microfluidic Electrode Integration with Conductive Ink

Journal:	<i>Lab on a Chip</i>
Manuscript ID	LC-COM-07-2020-000763.R1
Article Type:	Communication
Date Submitted by the Author:	28-Aug-2020
Complete List of Authors:	McIntyre, David; Boston University, Biomedical Engineering Lashkaripour, Ali; Boston University, Biomedical Engineering Densmore, Douglas; Boston University,

SCHOLARONE™
Manuscripts

Journal Name

ARTICLE TYPE

Cite this: DOI: 00.0000/xxxxxxxxxx

Rapid and Inexpensive Microfluidic Electrode Integration with Conductive Ink[†]

David McIntyre^{a,b}, Ali Lashkaripour,^{a,b} and Douglas Densmore^{b,c,*}

Received Date

Accepted Date

DOI: 00.0000/xxxxxxxxxx

Electrode integration significantly increases the versatility of droplet microfluidics, enabling label-free sensing and manipulation at a single-droplet (single-cell) resolution. However, common fabrication techniques for integrating electronics into microfluidics are expensive, time-consuming, and can require cleanroom facilities. Here, we present a simple and cost-effective method for integrating electrodes into thermoplastic microfluidic chips using an off-the-shelf conductive ink. The developed conductive ink electrodes cost less than \$10 for an entire chip, have been shown here in channel geometries as small as 75 μm by 50 μm , and can go from fabrication to testing within a day without a cleanroom. The geometric fabrication limits of this technique were explored over time, and proof of concept microfluidic devices for capacitance sensing, droplet merging, and droplet sorting were developed. This novel method complements existing rapid prototyping systems for microfluidics such as micromilling, laser cutting, and 3D printing, enabling their wider use and application.

Droplet microfluidics have enabled biochemical screening at single-cell resolution with unprecedented throughput, by encapsulating picoliter samples within an aqueous or non-aqueous emulsion.¹ The versatility of such platforms can be greatly improved with integrated electrodes, providing methods for sensing and manipulating the state of a single droplet (droplet position, size, etc.).² Label-free capacitance or impedance sensing can be integrated by placing two passive electrodes near one another to act as a capacitor.³ This has been used to track a single droplet's position, size, and velocity,⁴ monitor cell differentiation,⁵ and quantify DNA content in eukaryotic cells.⁶ Additionally, a local electric field generated by a high-voltage signal can be applied to overcome the stabilizing forces from added surfactants, merging adjacent droplets,^{7,8} or picoinjecting a stationary fluid into an adjacent passing droplet.⁹ High voltage signals

can also be pulsed at high frequencies (kHz-MHz range) to physically deflect polar, neutral droplets across streamlines in a non-polar continuous phase through dielectrophoresis, which can be used to build high-throughput droplet sorters.^{10–12} Effective implementation of these components greatly increases the potential impact of droplet microfluidics with applications across diverse fields such as synthetic biology,¹³ protein engineering,¹¹ and single cell analysis.¹⁴

Despite the profound potential of droplet microfluidics with integrated electrodes, adoption of these devices has been limited by expensive, manually intensive, and time-consuming fabrication methods. An ideal electrode integration method should be compatible with rapid prototyping, be affordable, and not present serious limitations to electrode geometries; however, currently no method fits all of these criteria (**Table 1**). Metal vapor deposition is a widely used electrode integration method, however this process is not scalable, needs accurate alignment, and requires a cleanroom facility.^{7,8} One major limitation to electrode geometries with current methods is the inability for dead-end filling, where electrode designs can be made with a "dead-end" (i.e. a channel that ends at a point). Without dead-end filling, electrode shapes are constrained to a path between an input and output. This significantly limits the complexity or number of electrodes by requiring additional ports, pumps, routing channels, and a bonding method with a high sealing pressure. Common flow-based integration methods using indium-based, low melting point solder¹⁵ and liquid metal,¹⁶ are both expensive and cannot be used for dead-end filling. Salt water electrodes are an affordable option,¹⁷ yet fabrication of electrodes requires a fluid source, input port, and output port. Moreover, the device substrate must be gas permeable (i.e. PDMS) for dead-end filling. This method is therefore potentially limiting in more scalable, rapid prototyping methods with desktop computer numerical control (CNC) micromilling,¹⁸ laser cutting,^{19,20} and 3-D printing,²¹ necessary when moving a device away from PDMS and into a more commercially-viable system.

Here, we present a novel electrode integration method for thermoplastic microfluidic chips using affordable, off-the-shelf, and carbon-based conductive ink (Bare Conductive Inc). This method

^a Boston University Biomedical Engineering Department, 44 Cummington Mall, Boston, USA.

^b Biological Design Center, 610 Commonwealth Ave, Boston, USA.

^c Boston University Electrical and Computer Engineering Department, 8 Saint's Mary St., Boston, USA. E-mail: dougd@bu.edu

[†] Electronic Supplementary Information (ESI) available. See DOI: 00.0000/00000000.

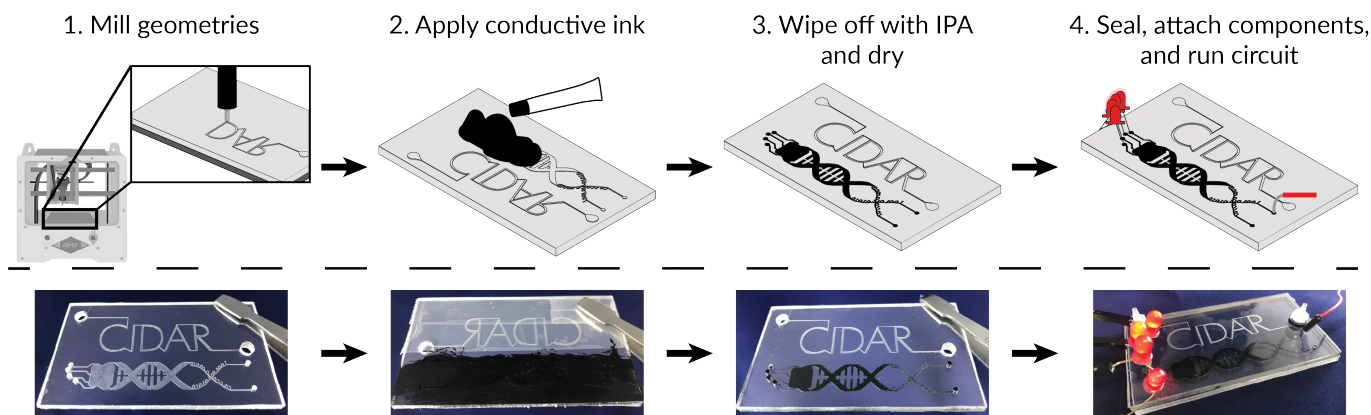


Fig. 1 Using conductive ink, electrodes can be integrated in minutes for less than \$10 for an entire device. The steps are as follows: (1) Electrode geometries are etched into a slab of polycarbonate with a desktop computer numerical control (CNC) micromill. (2) Conductive ink is applied over the entire area containing electrode geometries, and wiped on with tissue paper (Kimwipe). Any channels used for fluid flow are covered with tape to prevent nonspecific application. (3) Excess conductive ink is immediately removed with 91% isopropyl alcohol and left to dry for at least 15 minutes. Step 2 and 3 are repeated once, applying spot treatment as necessary. (4) Once dried, the device is sealed and the circuit can be assembled and tested.

directly complements previously reported rapid microfluidic prototyping workflows with desktop CNC micromilling, etching geometries as small as $75\ \mu\text{m}$ wide and $25\ \mu\text{m}$ deep into polycarbonate slabs.^{18,22} Electrodes have been successfully used in channels with a minimum dimension of $75\ \mu\text{m}$ wide and $50\ \mu\text{m}$ deep.

Once both fluid and electrode geometries are milled, conductive ink is applied to microfluidic chips with a simple “wipe on, wipe off” method (Figure 1). First, channels used for fluid flow are covered with tape (Scotch) to prevent contamination or possible clogging of the channels with conductive ink. Alternatively, electrode geometries can be etched onto the control layer. Conductive ink is applied onto the etched electrode geometries and wiped over the entire device using low-lint tissue wipes. Immediately after, another tissue covered in 91% isopropyl alcohol (IPA) is wiped over to remove excess conductive ink from the microfluidic chip. Remaining conductive ink is left to dry for at least 15 minutes and the process is repeated once with spot treatment as necessary. This electrode geometry then is attached to wire leads or any other circuit components through milled ports (Figure 2B). Components can also be attached prior to ink application for a more stable connection. All devices are sealed using an $81\ \mu\text{m}$ thick adhesive seal (Adhesives Research ArCare 90445). Once sealed, microfluidic devices are placed in a vacuum for at least 2 hours to expel any remaining air bubbles. The entire workflow, including fabrication, cleaning, electrode integration, and seal-

ing, is around 6-10 hours, depending on the complexity of the design.

To characterize the fabrication limitations and stability of conductive ink electrodes over time and ensure reproducibility when translating to prototypes, 1 cm straight-line electrodes ($N = 3$) were made across 60 different geometric combinations between $75\ \mu\text{m} \times 25\ \mu\text{m}$ and $397\ \mu\text{m} \times 397\ \mu\text{m}$ (Figure 2A). Smaller electrode widths and depths were not characterized due to fabrication limitations with desktop CNC micromilling, however, can be made with a more expensive mill. Accuracy of the channel width and depth was ensured by etching channels the same width as the endmills used and locally measuring the thickness of the polycarbonate slab after each tool change, respectively. After application of conductive ink, the performance of each electrode was then measured using an oscilloscope over a time-series by observing any attenuation of a 1.2 kV, 45 kHz sine wave pulsed at 1 kHz with a Lamp Upconverter (JKL Components BXA-12529), a waveform characteristic of active manipulations in droplet microfluidics (Figure 2B).¹² Electrodes were deemed “conductive” if the amplitude of the measured waveform after being passed through a conductive ink electrode was the same as the input amplitude (1.2 kV). Any reduction of waveform amplitude resulted in deeming the electrode “not conductive.”

Immediately after application, all electrodes were conductive other than those $25\ \mu\text{m}$ deep; this did not change for the next 24 hours (Figure 2C, first graph). Electrode $25\ \mu\text{m}$ deep failed from conductive ink being physically removed from the channel after wiping off with IPA. At one week, four of the $50\ \mu\text{m}$ deep electrodes were not conductive and one of the $75 \times 200\ \mu\text{m}$ channels failed (Figure 2C, second graph): this was due to physical breaks in the electrodes or a disconnection from the inserted leads. For a longer time-series, a subgroup of geometries similar to those used in the proof-of-concept applications (100, 125, and $150\ \mu\text{m}$ wide, all depths) were tested up to one month (Figure 2C, third graph). After 1 month, all channels greater than 50

Table 1 Comparison of common methods for integrating electrodes into droplet microfluidics. Electrode cost does not include that of the device substrate.

	Cost (\$/mL)	Resistivity ($\Omega \cdot \text{cm}$)	Dead-end Filling	Immediate Use
Low-mp Solder	171.78	8.4×10^{-6}	No	Yes
Liquid Metal	74.5	2.9×10^{-5}	No	Yes
Salt Water (5M)	0.01	4.4	Limited	No
Conductive Ink	0.325	0.28	Yes	Yes

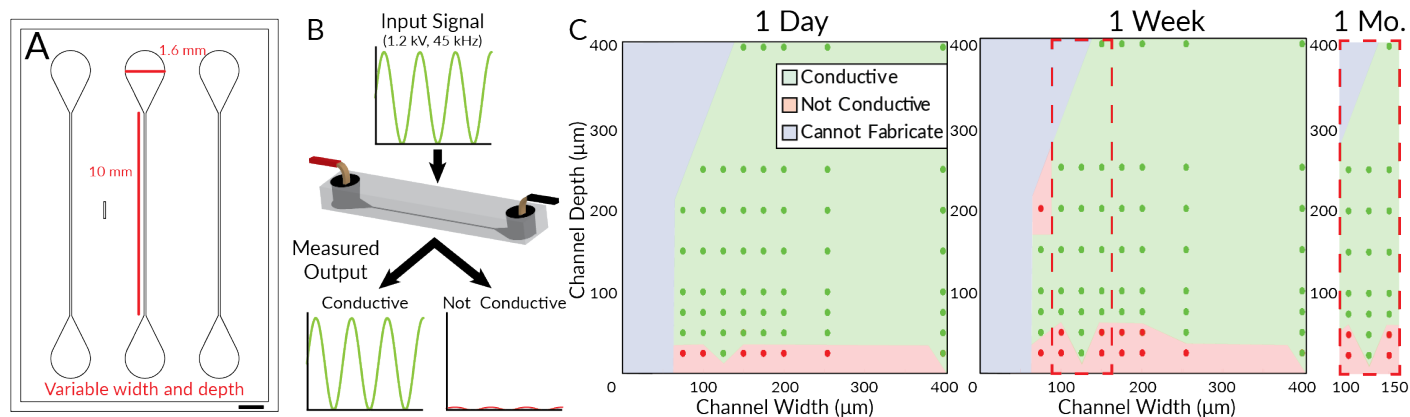


Fig. 2 Physical characterization of electrodes demonstrates a wide range of channel widths and depths that are stable for at least 1 month. (A) Electrode stability was tested across 60 different geometries batched onto multiple chips, ranging from $75 \mu\text{m} \times 25 \mu\text{m}$ to $397 \mu\text{m} \times 397 \mu\text{m}$. In all designs, lead connection diameter and channel length were kept constant at 1.6 mm and 10 mm, respectively. Scale bar is 1 mm. (B) Performance of each electrode was characterized by measuring any attenuation after passage of a high-voltage, high-frequency signal through the electrode. (C) This was characterized across all geometries for up to 1 week, and in a subgroup of electrodes up to 1 month. All electrodes were kept at room temperature.

μm deep within this range were still conductive with no signal attenuation, giving stable, reliable operating conditions for conductive ink electrodes in droplet microfluidics. Electrode stability was not measured past this time point. A more robust connection to wire leads may improve the performance of the failed, smaller geometries, however, these were not needed to develop functional proof-of-concept applications. By keeping electrode geometries within the stable design parameters identified, reproducible performance across each device prototype can be ensured with a minimum shelf-life of 1 month. Long-term use of these electrodes does not require any involved user steps, all the user needs to do is connect the inserted wire leads to the rest of the circuitry. Such performance is currently not possible unless using methods 2-3 orders of magnitude more expensive.^{7,15,16}

To test the feasibility of this method in practice, electrodes were fabricated and tested across common applications in droplet microfluidics: droplet capacitance sensing, merging, and sorting (Figure 3). All proof-of-concept devices were also simulated with a 2D model in COMSOL Multiphysics 5.4 in order to visualize the electric field. Simulations were modeled using the different relative permittivities of water, mineral oil, HFE-7500 fluorinated oil, and polycarbonate ($\epsilon_{\text{water}} = 80.12$, $\epsilon_{\text{oil}} = 2.8$, $\epsilon_{\text{HFE}} = 5.6$ and $\epsilon_{\text{pc}} = 3$). All simulations are available at github.com/CIDARLAB/electrical-integration. Fluid flow in proof of concept devices was controlled with syringe pumps (Harvard Apparatus). Images were captured using a high-speed camera (IDT X-Stream) attached to a stereo microscope (Amscope). An 18,000 lumen LED light source (Expert Digital Imaging) was directly underneath each microfluidic device for proper illumination at higher frame rates. Droplets were generated upstream of the specific component with a size and generation rate dependent on the application.

Capacitance sensing is a label-free and simple method of tracking and identifying significant material differences between droplets, requiring only passive electrodes and an off-the-shelf capacitance-to-digital converter for measurement (AD7746, Ana-

log Devices). When electrodes are placed across from another on either side of the channel, they act as a "parallel plate" capacitor with two materials in between. Capacitance change between these electrodes can be calculated using the following equation:

$$C_{\text{tot}} = \left(\frac{2}{C_{\text{pc}}} + \frac{1}{C_{\text{fluid}}} \right)^{-1},$$

where C_{pc} and C_{fluid} are the capacitance of the polycarbonate and fluid, respectively. Water and mineral oil have significantly different relative permittivities ($\epsilon_{\text{water}} = 80.12$, $\epsilon_{\text{oil}} = 2.8$), and therefore will result in different capacitance measurements between the passive electrodes. When a positive voltage is applied, the effective electric field is lower in water than oil as water dipole moments are polarized in the opposite direction to the potential difference, thus increasing the capacitance as the electrodes with water can store more charge (Figure 3A, column 3).

Using conductive ink electrodes, colored DI water droplets in mineral oil containing 5% V/V Span 80 surfactant (Sigma Aldrich) were detected at a range of droplet generation frequencies between 1 - 2.5 Hz (Figure 3A, column 4; Video S1). Accuracy of these measurement were validated by comparing measured signal against pixel intensity measurements of the region in between the two electrodes across 5 seconds. Image analysis was done using ImageJ (Fiji). Both the capacitance and pixel intensity measurements were smoothed with a 5-point rolling average and normalized by its minimum and maximum values. Higher throughput and more sensitive capacitance sensing was limited by the capacitance-to-digital converter used: the maximum sampling rate of the AD7746 is 90.9 Hz, and as the noise increases with sampling rate, at sampling rates above the 16.1 Hz used noise is too high to discriminate the capacitance change from a passing droplet. Capacitance sensing can be improved with more specialized capacitance to digital converters or an impedance amplifier, with little to no change needed in the electrode design. With this improved circuitry and increased number of electrodes, this system can be extended to measure the size, velocity, and

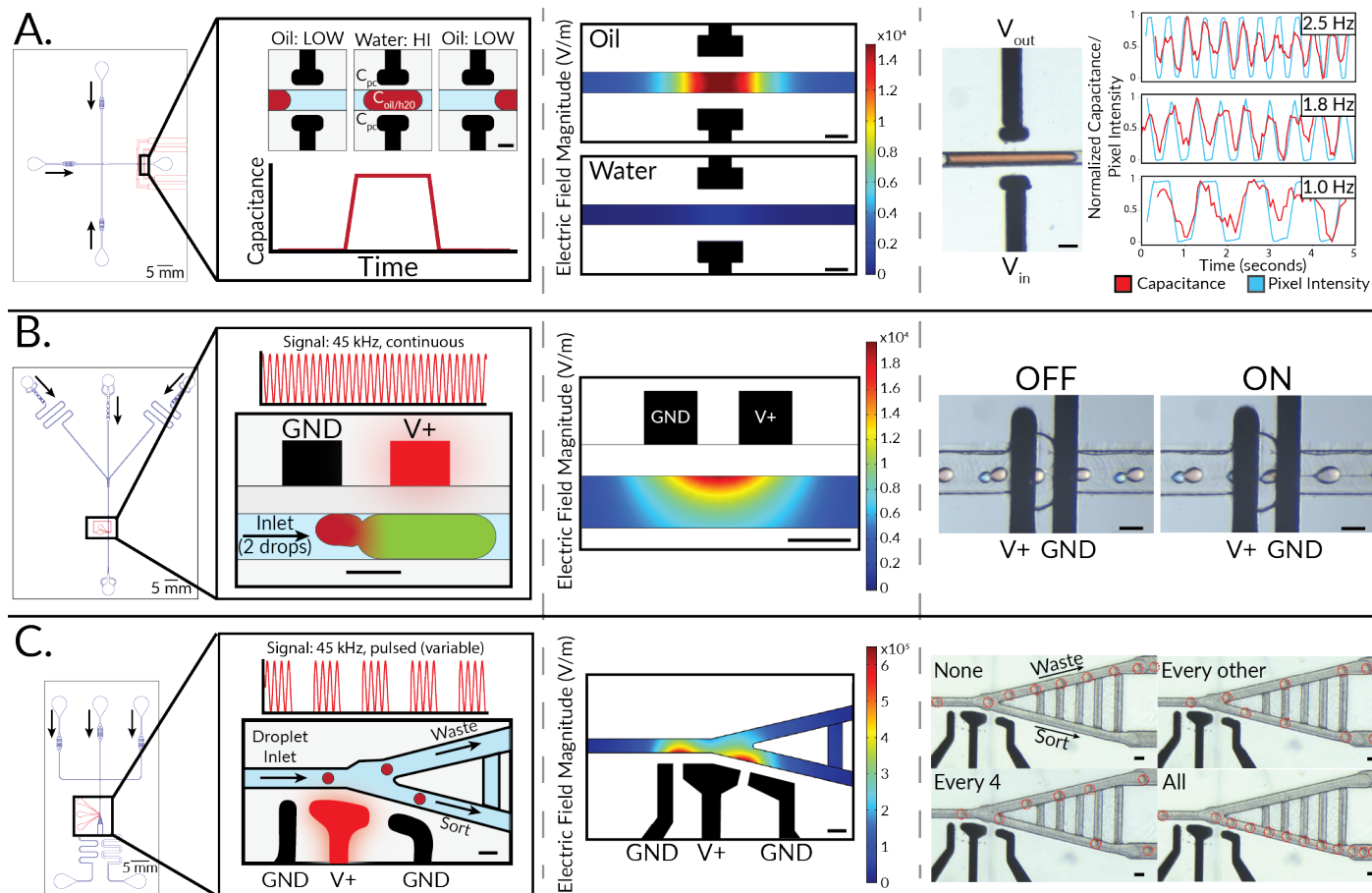


Fig. 3 Proof-of-concept applications of integrated conductive ink electrodes. (A) Capacitance sensing was successfully integrated to discriminate between droplets produced at differing generation rates. (B) A constant signal was delivered to enable droplet merging at up to 80 Hz (35 Hz merging between droplets 175 μm and 75 μm are shown). (C) A signal was selectively delivered to a single electrode for droplet sorting. The periodicity of signal delivery was manually tuned to deflect different fractions of all 100 μm droplets generated at 130 Hz with no false positives. Videos of each proof-of-concept are provided in the supplementary information. Scale bars are 125 μm unless labeled otherwise.

specific content of a passing droplet.⁴

A more challenging task is active manipulation of droplet state, requiring passing a high-voltage, high-frequency signal to a target area. Successful signal delivery to the end of the electrode can be limited by signal dissipation and reduced bandwidth from materials with high resistivity. Although the resistivity of conductive ink is orders of magnitude higher than metal-based electrodes, it is less than that of salt water, which has been used previously for similar applications and shown in simulation to not result in significant attenuation.¹⁷ Active signal delivery was first tested by inducing droplet merging. A local electric field generated by a high-voltage, high-frequency signal can induce merging between two droplets in physical contact by disrupting the stabilizing forces from surfactants (Figure 3B, 3rd column). Electrodes were placed on another polycarbonate layer separated by the adhesive seal. Using a 1.2 kV, 45 kHz signal continuously switched on and off at 1 kHz, colored DI water droplets in mineral oil containing 5% V/V Span 80 surfactant (Sigma Aldrich) were successfully merged at a range of frequencies between 12 Hz and 80 Hz (Figure 3B, 4th column, Video S2). Any unsuccessful merging was due to adjacent droplets not being in close enough proximity. Merging above 80 Hz was limited by inaccurate pair-

ing of droplets upstream, not electrode performance. Accurate droplet merging enables sequential reagent addition, making it a fundamental component to performing complex molecular biology operations in droplet microfluidics at high throughput.

The final proof-of-concept developed was a droplet sorter. To accurately sort droplets, electrodes are needed to selectively deliver a high-voltage signal to a single droplet that generates a brief local electric field that dielectrophoretically deflects it across streamlines into a "keep" channel (Figure 3C, 2nd & 3rd column). In dielectrophoresis, a dielectric force is generated by inducing a dipole moment in a polar droplet in a non-uniform field.²³ The generated force (F_{DEP}) is expressed as:

$$F_{DEP} = \bar{m} \nabla \vec{E},$$

where \bar{m} and $\nabla \vec{E}$ are the dipole moment of the droplet and the electric field gradient, respectively. An AC field is applied to limit electric-field screening effects. Droplets without target characteristics are not deflected and continue along into the "waste" channel due to fluidic resistance differences between each output. Accurate sorting requires effective coupling between sensors and actuators and a quick enough propagation time of a signal to

the end of the electrode to accurately deflect a droplet. Actuation must also be controlled enough such that adjacent droplets are not non-specifically deflected. Droplet sorting was tested through controlled deflection (every other, every 4th, etc.) of 100 μm colored DI water droplets in fluorinated Droplet Generation Oil (Biorad) up to 130 Hz (Figure 3C, 4th column, Video S3). Droplets were selectively sorted with a user-defined waveform from a function generator pulsing a 1.2 kV, 45 kHz sine wave on and off. This droplet sorter is a cheap and easy to integrate system in thermoplastic microfluidic device, while still delivering a relevant throughput.

Conclusions

We have shown here a novel electrode integration method with thermoplastic microfluidic chips using carbon-based conductive ink. This is the first method to the extent of our knowledge that is less than \$1 per device, simple to fabricate, and allows for dead-end electrode designs in thermoplastics. Conductive ink electrodes are highly suitable for rapid prototyping of microfluidic devices in thermoplastics, and has the potential for use at the industrial scale when coupled to a higher-throughput application method such as inkjet or screen printing. This system has been used for droplet capacitance sensing, merging, and sorting in thermoplastic chips. We believe these proof-of-concept applications are the first of such performance shown within cost-effective thermoplastic droplet microfluidic devices. Integration does not have to be limited to such applications: conductive ink electrodes can be used for any application of electrodes in microfluidics, such as picoinjection of an adjacent continuous flow. This method could also be extended to other rapid prototyping methods, such as 3D printing²⁴ or laser cutting,^{19,20} further advancing the sophistication of cleanroom-free microfluidic devices.

Despite these substantial advantages, a few properties limit its universal use. Channels made for fluid flow must be covered during conductive ink application to prevent nonspecific application, which becomes more difficult as the design geometries become smaller. While this can be solved by having electrodes on the supporting polycarbonate layer, the thickness of the substrate used for bonding (PDMS, adhesive, etc.) must be accounted as this reduces the magnitude of the local electric field and some alignment is needed. However, these limitations are minor compared to those imposed by existing methods. Conductive ink electrodes are an affordable option for integration into thermoplastic microfluidic chips, compatible with dead-end filling and not requiring a cleanroom, expanding the availability of sophisticated, rapidly developed droplet microfluidic devices.

Author Contributions

D.M. fabricated all devices, performed experiments and data analysis, and was the lead author on the paper. Both D.M. and A.L. conceptualized the research idea and designed experiments. A.L. designed the droplet merger. D.D. supervised this work. All authors helped prepare the manuscript.

Acknowledgements

The authors would like to thank Prof. Rabia Yazicigil, Radhakrishna Sanka, and Shachi Khadilkar for their help in circuit design and PCB fabrication. This work was supported by the NSF Living Computing Project Award 1522074.

Conflicts of interest

There are no conflicts to declare.

Notes and references

- 1 M. T. Guo, A. Rotem, J. A. Heyman and D. A. Weitz, *Lab on a Chip*, 2012, **12**, 2146.
- 2 X. Niu, M. Zhang, S. Peng, W. Wen and P. Sheng, *Biomicrofluidics*, 2007, **1**, 1–12.
- 3 J. Z. Chen, A. A. Darhuber, S. M. Troian and S. Wagner, *Lab on a Chip*, 2004, **4**, 473–480.
- 4 P. K. Isgor, M. Marcali, M. Keser and C. Elbuken, *Sensors and Actuators B: Chemical*, 2015, **210**, 669–675.
- 5 W. Fan, X. Chen, Y. Ge, Y. Jin, Q. Jin and J. Zhao, *Biosensors and Bioelectronics*, 2019, **145**, year.
- 6 L. Sohn, O. Saleh, G. Facer, A. Beavis, R. Allan and D. A. Notterman, *Proceedings of the National Academy of Sciences*, 2000, **97**, 10687–10690.
- 7 K. Ahn, J. Agresti, H. Chong, M. Marquez and D. A. Weitz, *Applied Physics Letters*, 2006, **88**, 264105.
- 8 C. Priest, S. Herminghaus and R. Seemann, *Applied Physics Letters*, 2006, **89**, 134101.
- 9 A. R. Abate, T. Hung, P. Mary, J. J. Agresti and D. A. Weitz, *Proceedings of the National Academy of Sciences of the United States of America*, 2010, **107**, 19163–6.
- 10 K. Ahn, C. Kerbage, T. P. Hunt, R. M. Westervelt, D. R. Link and D. A. Weitz, *Applied Physics Letters*, 2006, **88**, 024104.
- 11 J. J. Agresti, E. Antipov, A. R. Abate, K. Ahn, A. C. Rowat, J.-C. Baret, M. Marquez, A. M. Klibanov, A. D. Griffiths and D. A. Weitz, *Proceedings of the National Academy of Sciences*, 2010, **107**, 4004–4009.
- 12 H.-D. Xi, H. Zheng, W. Guo, A. M. Gañán-Calvo, Y. Ai, C.-W. Tsao, J. Zhou, W. Li, Y. Huang, N.-T. Nguyen and S. H. Tan, *Lab on a Chip*, 2017, **17**, 751–771.
- 13 P. C. Gach, K. Iwai, P. W. Kim, N. J. Hillson and A. K. Singh, *Lab on a Chip*, 2017, **17**, 3388–3400.
- 14 E. Brouzes, M. Medkova, N. Savenelli, D. Marran, M. Twardowski, J. B. Hutchison, J. M. Rothberg, D. R. Link, N. Perrimon and M. L. Samuels.
- 15 A. C. Siegel, S. S. Shevkoplyas, D. B. Weibel, D. A. Bruzewicz, A. W. Martinez and G. M. Whitesides, *Angewandte Chemie International Edition*, 2006, **45**, 6877–6882.
- 16 J. H. So and M. D. Dickey, *Lab on a Chip*, 2011, **11**, 905–911.
- 17 A. Sciambi and A. R. Abate, *Lab Chip*, 2014, **14**, 2605–2609.
- 18 A. Lashkaripour, R. Silva and D. Densmore, *Microfluidics and Nanofluidics*, 2018, **22**, 31.
- 19 T. Trantidou, M. S. Friddin, K. B. Gan, L. Han, G. Bolognesi, N. J. Brooks and O. Ces, *Analytical chemistry*, 2018, **90**, 13915–13921.
- 20 H. Klank, J. P. Kutter and O. Geschke, *Lab on a Chip*, 2002, **2**, 242–246.
- 21 C. M. B. Ho, S. H. Ng, K. H. H. Li and Y.-J. Yoon, *Lab on a Chip*, 2015, **15**, 3627–3637.
- 22 A. Lashkaripour, C. Rodriguez, L. Ortiz and D. Densmore, *Lab on a Chip*, 2019, **19**, 1041–1053.
- 23 R. Pethig, *Biomicrofluidics*, 2010, **4**, 022811.
- 24 A. K. Au, W. Huynh, L. F. Horowitz and A. Folch, *Angewandte Chemie International Edition*, 2016, **55**, 3862–3881.

Electrode integration with off-the-shelf conductive ink provides a rapid and cost-effective method to develop sophisticated microfluidic prototypes in thermoplastics.

